Low-cost Terrestrial Laser Scanners for Permanent Monitoring of Beach-Dune Systems

Daan Hulskemper[1,*], Hannah Weiser[2,3], Ronald Tabernig[2,3], Bernhard Höfle[2,3], Thomas de Jong[1], Roderik Lindenbergh[1]

[1]Dept. of Geoscience and Remote Sensing, Faculty of Civil Engineering and Geoscience, Delft University of Technology, The Netherlands – (d.c.hulskemper, r.c.lindenbergh)@tudelft.nl, t.m.s.dejong@student.tudelft.nl
[2]3DGeo Research Group, Institute of Geography, Heidelberg University, Germany – (h.weiser, ronald.tabernig, hoefle)@uni-heidelberg.de
[3]Interdisciplinary Center for Scientific Computing (IWR), Heidelberg University, Germany

Keywords: Permanent laser scanning, sandy beach dune systems, simulations, virtual laser scanning, low cost, 3D

Abstract

Permanent laser scanning (PLS) is an effective tool for near-continuous monitoring of topographical changes in beach-dune systems. While PLS systems were traditionally costly, the emergence of affordable LiDAR sensors enables larger-scale setups with multiple scanners or sites. However, the different characteristics compared to high-end devices, create challenges for one-on-one replacement. To assess how low-cost sensors can replace high-end sensors, we compare the performance of a setup with several low-cost Livox AVIA sensors to a single high-end RIEGL VZ-2000i sensor in its ability to capture an embryonic dune field with large variation in topography. This is evaluated using HELIOS++ virtual laser scanning (VLS). To also assess the representativeness of the simulations, we further compare the VLS to real-world measurements with the Livox AVIA. Based on a VLS setup with six AVIAs mounted on tripods at 2 m above ground, a coverage of 52% can be obtained, which is similar to the coverage of a single RIEGL VZ-2000i on a tower 8 m high. The real-world experiments confirm the VLS results with a slightly lower point cloud coverage of 42%. Furthermore, the effective range of the Livox AVIA in a beach-dune system lies around 100-150 m. At larger ranges, only pulses at high incidence angles (angle between surface and incoming beam, $>20^o$) are registered at the scanner. The variations in coverage between the VLS and real-world scans highlight the need for careful consideration of the occlusion potential of different representations of the topography, beam divergence shapes, and the moisture conditions.

1. Introduction

Permanent 3D monitoring, also known as Permanent Laser Scanning (PLS), provides a powerful means to analyse short-term sand transport processes and their interactions with longer-term morphological changes in coastal environments (Anders et al., 2021; Kuschnerus et al., 2024; Lindenbergh et al., 2025a). Such continuous observations, rather than intermittent measurements, enhance our understanding of both natural and anthropogenic influences on coastal dynamics, which often manifest as high-frequency, small-scale disturbances to coastal sediment budgets (Hulskemper et al., 2026).

PLS systems have so far been primarily applied at single study sites. However, coastal systems are inherently complex, and small variations in environmental conditions, such as wind speed, tide level, or moisture content, can lead to large variations in geomorphological response (Chowdhury et al., 2023). Consequently, deploying PLS setups across broader and more diverse coastal areas would substantially improve our understanding of these spatially and temporally variable processes. Yet the high cost of conventional LiDAR instruments remains a major limitation, restricting the implementation of multi-site or large-scale monitoring networks.

Recent advances in low-cost LiDAR technology offer promising alternatives that could make distributed PLS applications feasible (Bi et al., 2021). Devices such as the Livox AVIA provide affordable and lightweight options, but their performance characteristics differ significantly from high-end systems (Ruttner-Jansen et al., 2023). Differences in beam divergence, effective range, scanning pattern, and field of view (FOV) mean that low-cost scanners cannot simply replace high-end instruments without compromising coverage or data quality (Soudarissanane et al., 2011). To effectively integrate such sensors into coastal monitoring systems, it is therefore essential to quantify their capabilities and limitations, and to determine how setups can be designed to complement or substitute traditional scanners.

Virtual Laser Scanning (VLS) provides a valuable framework for this evaluation and the design of monitoring campaigns (Winiwarter et al., 2022; Tabernig et al., 2025a), as it enables the simulation and analysis of scanner performance (coverage and point density) under controlled conditions with the option to run a high number of survey and scene scenarios with varying sensor settings. However, for accurate incorporation and use of new simulated low-cost scanners, these simulations must be validated through field measurements to ensure reliability and practical relevance.

In this study, we aim to combine VLS with real-world measurements to assess the feasibility of using multiple low-cost scanners as an alternative to a single high-end instrument for permanent beach-dune monitoring. We assess the differences between VLS simulations and real-world application of these low-cost sensors, to provide aid in the use of VLS for setup design, and feasibility of low-cost sensors for permanent monitoring of beach-dune systems. Specifically, we address the research questions:

RQ1 How does the coverage, point density, and scanning angle of a PLS setup with multiple low-cost Livox AVIA scanners compare to a setup with a single high-end laser scanner?

* Corresponding author

RQ2 How does the coverage, point density, and scanning angle of simulated low-cost acquisitions compare to their real-world performance?

To answer these questions, we design and compare a low-cost and high-end scanner setup in an embryonic dune field on the Zandmotor (The Netherlands, De Schipper et al., 2016), a dynamic coastal environment characterized by high spatial and temporal variability in topography. The performance of each setup is analysed in terms of coverage, point density, and incidence angle, using both HELIOS++ virtual scanning and field validation. The variations in roughness (and related precision) between the scans are not assessed, as this requires even more sophisticated modelling of laser scanning error propagation and virtual terrain reconstruction. For the low-cost setup we use a Livox AVIA scanner, whereas for the high-end setup a widely used PLS system, the RIEGL VZ-2000i, is used. This study focuses on the performance of one high-end laser scanner compared to multiple low-cost scanners. Elsewhere in De Vugt et al. (2025), a similar comparison has been made, but focussing on change detection from close-range (∼20 m) single scanners in a multi-epoch approach.

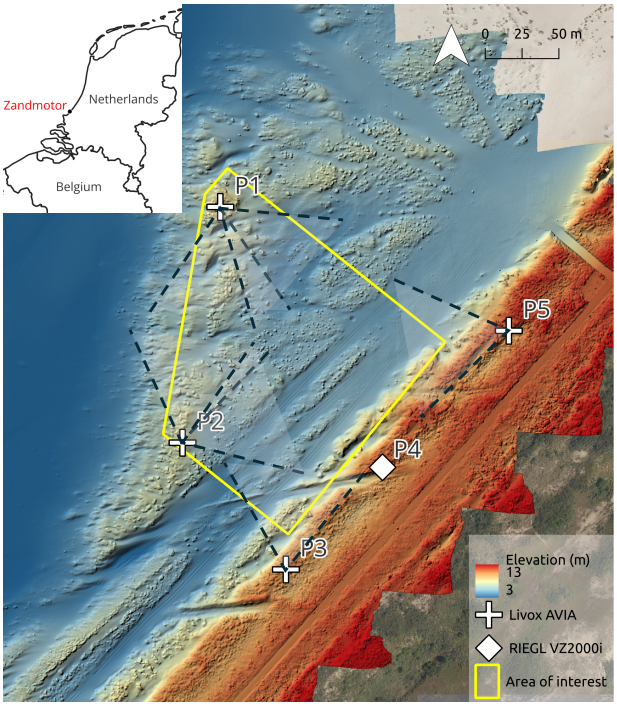

Figure 1. Scan area to be covered by 1 high-end laser scanner or 6 low-cost laser scanners. Visualized point cloud is obtained by UAV-LiDAR (ULS) and colored by elevation. The field-of-views per scan position and direction are indicated with dashed lines. Background aerial imagery is from pdok/beeldmateriaal.nl. The subfigure shows the location of the Zandmotor in The Netherlands.

2. Materials

2.1 Study area

The study area under consideration is an embryonic dune field on the *Zandmotor* in The Netherlands (Figure 1). This is part of a mega-nourishment project, where in 2011 millions of cubic meters of sand have been placed at once, to investigate how the sand would disperse and how the area itself would evolve (Stive et al., 2013). In the last 15 years, around half of the initial *Zandmotor* has been colonised by small embryonic dunes with heights up to ∼8 m, creating a topography with a lot of local variation in elevation (Hulskamp et al., 2025). This makes it complex to monitor from fixed positions without occlusion. The juvenile dunes in the study area show large variations in orientation and sand volume over short-time spans ($<$ months) under varying environmental conditions (Lindenbergh et al., 2025b). These factors together make it an ideal study case for assessing the use of low-cost LiDAR scanners.

2.2 Livox AVIA

The low-cost LiDAR scanner under consideration is the Livox AVIA. This is a lightweight scanner, which comes at a relatively low-cost. According to the specifications (LIVOX AVIA User Manual, 2020), the scanner is able to emit 240,000 points per second, and receive triple returns. The beam divergence (Full Width at Half Maximum, FWHM) is 0.28° (vertical) × 0.03° (horizontal), creating a horizontally narrow beam. In non-repetitive scanning mode, the scanner works in a rotating 4-petalled flower-shaped pattern (Figure 2), with an effective field-of-view (FOV) of 70.4° horizontally and 77.2° vertically. As the ellipsoid of the FOV only slowly fills up with repeated cycles, the scanning duration has great influence on the point density and coverage. Figure 2 shows the coverage over the FOV for different scanning periods. The ranging precision is 2 cm according to specifications (σ at 20 m).

2.3 RIEGL VZ-2000i

The high-end scanner we consider is a RIEGL VZ-2000i. This is a large terrestrial laser scanner, with 360° horizontal and 100° vertical FOV (Riegl VZ-2000i Data sheet, 2019). Its beam divergence is circular with at maximum 0.0155° (at $1/e^2$), but this can be adapted depending on required performance. The ranging precision is 3 mm according to specifications (σ at 100 m). The sensor and its predecessors have been widely employed in permanent environmental laser scanning setups (e.g. Kuschnerus et al., 2021a; Schröder et al., 2022), particularly because of their long range of up to 2,500 m. These previous applications typically relied on single-scanner PLS configurations (Vos et al., 2022, 2023). In this study, the RIEGL VZ-2000i is used only in virtual form, with its performance simulated in the HELIOS++ software.

2.4 Digital representation of scan area with UAV LiDAR

The study area has been surveyed by means of a DJI Matrice 300RTK equipped with a Yellowscan Mapper+ LiDAR sensor, to create a point cloud that fully covers the area. This point cloud is then used to obtain virtual laser scans to simulate performance differences between high-end and low-cost scanners, and to gain information on the difference in performance between virtual scanning and real-world scanning. The UAV LiDAR (ULS) point cloud is acquired from 70 m above ground, with an overlap factor of 0.5. This results in a point density of ∼600 points/m^2.

To enable simulation and reduce computation time, the ULS point cloud is converted to a simplified surface representation before simulation in HELIOS++ (Section 3.2). This is done in two ways to study the effect of different representations on performance of the simulations. One representation is acquired by spatial subsampling of the point cloud with a minimum length

This contribution has been peer-reviewed. The double-blind peer-review was conducted on the basis of the full paper.
https://doi.org/10.5194/isprs-annals-XI-1-2026-91-2026

of 0.25 m. Then, using a 2D Delaunay triangulation with a maximum edge length of 2 m, a mesh (OBJ format) is created. This representations is optimistic in the sense that some high elevation points that in reality interfere with the laser beams may be filtered out. The second representation is a more pessimistic raster representation (GeoTIFF format), as it uses the maximum elevation value of the original point cloud per grid cell, with a cell size of $0.1 \times 0.1\ m^2$. This should represent the worst case scenario in terms of occlusion.

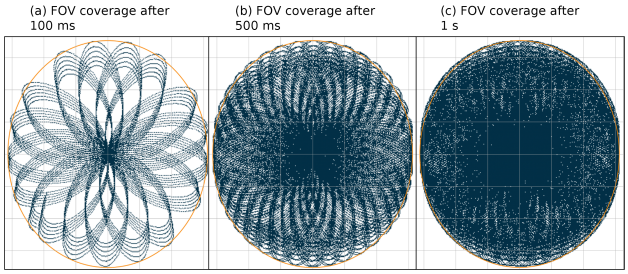

Figure 2. Coverage of the field of view (FOV) of the Livox AVIA after 100 ms, 500 ms and 1 s, resp. Coverage is based on real scanning data.

3. Methods

To assess the variation in performance and characteristics of a high-end vs. a low-cost PLS setup, and virtual vs. real world laser scanning we design two fieldwork configurations, one high-end and one low-cost. Using these two configurations and the digital representation of the study area we run virtual laser scanning simulations with HELIOS++ (Winiwarter et al., 2022). The low-cost configuration is further verified by acquiring real-world scans. The performance of the various scan configurations is assessed by computing the following comparison metrics: coverage, point density, incidence angle, roughness.

3.1 Fieldwork setup design

We design a fieldwork setup that covers the area of interest (AOI) as visible in Figure 1. The fieldwork was performed on 2025-10-21. The setup contains two scenarios. The first scenario uses four Livox AVIA scanning positions, at a height of 2 m above the topography, i.e., the height of a tall tripod. This scenario is scanned both using virtual laser scanning (LIVOX-VLS) and the actual Livox AVIA (LIVOX-REAL). Here we aim to closely replicate the LIVOX-REAL scans with the LIVOX-VLS simulations. The second scenario (RIEGL-VLS) is only virtually scanned, and uses a RIEGL VZ-2000i at a single tower of 8 m.

The in-situ (LIVOX-REAL) measurements are acquired as follows. The area is initially scanned using ULS. Resulting point clouds are georeferenced to the RDNew (De Bruijne et al., 2005) coordinate system using onboard GNSS data. Next, a single Livox AVIA sensor is used to consecutively scan the AOI from the predefined viewpoints. The locations are chosen such that they are at the highest local topography, on top of embryonic dunes. From positions P1 and P2 we scan in two directions, such that the full AOI is covered in theory (Figure 1). The six scans are co-registered to the ULS data in *CloudCompare* using manual point picking of dune crests for coarse alignment, followed by subsampling of all clouds (0.2 m) and fine alignment with the Iterative Closest Point (ICP) algorithm.

3.2 Virtual laser scanning with HELIOS++

HELIOS++ is an open-source software for simulating LiDAR point clouds from different platforms, a variety of scanner models, and for any given 3D input scene (Winiwarter et al., 2022). This makes HELIOS++ a powerful tool for planning and comparing laser scanning acquisition strategies in a controlled environment, which supports decision-making for real-world field campaigns. For the simulations, we built a digital replica of the study area, which serves as the virtual input scene (Section 2.4).

The two scanners, Livox AVIA and RIEGL VZ-2000i, are implemented based on the scanner datasheets. Since the beam divergence of the Livox AVIA (LIVOX-VLS) is highly elliptical, and HELIOS++ currently only supports circular beam divergence, we perform simulations with both *a*) the semi-minor axis (0.03^o) and *b*) the mean of the semi-minor and the semi-major axis (0.155^o). For LIVOX-VLS, we simulate acquisition times of 20 seconds per scan position, which can be filtered by time to also obtain point clouds for shorter integration times. The maximum range is limited to 150 m, which is approximately the range up to which points can be reliably detected in the real-world dataset. For each version, we merge the six scans and retain the point source IDs.

The RIEGL VZ-2000i is simulated according to settings used previously at other PLS stations for beach monitoring (Vos et al., 2023). Namely, with 0.03° horizontal and vertical scan resolution, 300 kHz pulse repetition rate (PRR) and maximum possible FOV (Section 2.3). The output consists of a single simulated point cloud.

3.3 Comparison metrics

We compare the point cloud characteristics in terms of **point density**, **coverage**, and **incidence angle**, between the LIVOX-REAL, LIVOX-VLS (with beam divergence *a* and *b*), and the RIEGL-VLS point clouds. For LIVOX-VLS we also compare different scanning durations. As the area of interest shows smooth local topographical variations but no steep or vertical surfaces, all metrics are computed on a 2D grid of the AOI with a cell size of $0.25 \times 0.25\ m^2$.

The **point density** and **coverage** are derived by counting the number of points per 0.25 m raster cell based on their X and Y coordinates. A cell is considered covered if at least one point falls within it. Point density is then obtained by dividing the number of points in a cell by the cell area.

To compute the **incidence angle** we fit local planes to the surface. These planes are based on all points that fall in each grid-cell in the ULS point cloud. For each grid cell, a plane is fitted through the surrounding points using their covariance matrix. The third eigenvector of this matrix represents the surface normal. The **incidence angle** is then derived from the ULS point cloud surface by calculating the angle between this normal and the vector from each scanning position to the cell center. Subtracting this value from 90° gives the angle between the surface and the incoming beam.

4. Results

The results are presented in three steps: (1) variation in LIVOX-VLS performance with scan duration, beam mode, and digital representation; (2) comparison with the high-end RIEGL VZ-2000i; and (3) differences between simulated and real-world Livox data.

This contribution has been peer-reviewed. The double-blind peer-review was conducted on the basis of the full paper.
https://doi.org/10.5194/isprs-annals-XI-1-2026-91-2026 | © Author(s) 2026. CC BY 4.0 License.

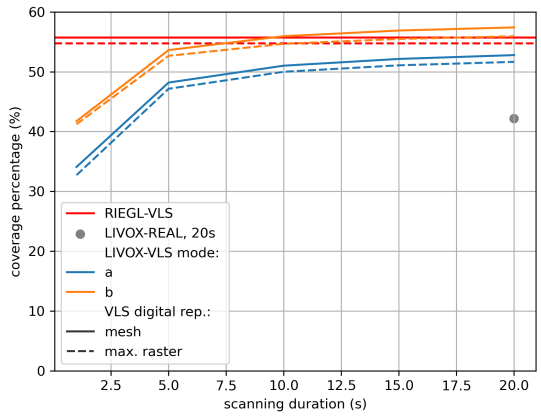

Figure 3. Coverage vs. scanning duration for the simulated Livox AVIA, in beam mode *a* (semi-minor axis beam width) and *b* (average between semi-minor and semi-major axis beam width), for the two digital representations. The coverage of the simulated RIEGL VZ-2000i is indicated in red, this does not mean that the RIEGL scans instantaneously at maximum coverage–it scans for several minutes.

4.1 Influence of integration time, beam width, and digital representation

As a consequence of its scanning pattern (Figure 2), the performance of the Livox AVIA largely depends on the scanning duration. In Figure 3 we plot the coverage vs. the scanning duration for the LIVOX-VLS scenario. The coverage increases with duration, but the slope decreases at higher durations, seemingly approaching an asymptote.

The simulated beam scenario has large influence on the coverage percentage. When simulating a circular divergence equal to the semi-minor axis (0.03^o; mode a), the total coverage was 51%, compared to 56% when using the mean divergence (0.155^o; mode b).

The two digital representations of the scene produce small but systematic differences. The maximum raster representation results in a lower coverage (by $\sim$2 %), possibly due to increased occlusion. The real-world scan (LIVOX-REAL) achieves an even lower coverage of 42%, indicating that real surface characteristics such as small-scale roughness and surface moisture further reduce effective returns compared to the virtual representations.

4.2 Comparison of low-cost and high-end setups

The low-cost and high-end simulated setups obtain a similar coverage of around 50-55% of the AOI (Table 1). The difference lies in the mean point density, which for the Livox AVIA is at least four times as high as for the RIEGL-VLS.

If we compare the spatial trends in coverage and point density of the Livox AVIA vs. the RIEGL VZ-2000i, it becomes apparent that the AVIA setup creates large spatial regions without data, particularly in low-lying areas, at longer ranges, and behind dune crests (Figure 4). However, when it captures a region, it does so with a more homogeneous point density (Figure 5). This is the result of overlapping FOVs from different scanning, and the non-repetitive scan pattern over a single FOV during 20 s of scanning. Compare the region in the north-west of the study area in Figure 4a. Both LIVOX-VLS and LIVOX-REAL show gaps, whereas the RIEGL obtains data, but with a relatively low point density compared to regions closer to the scanner (Figure 5d). The RIEGL thus seems better able to acquire points at longer ranges, behind dune crests, and at lower incidence angles. The latter is also confirmed by the lower average incidence angle (Table 1), which indicates that it gets more returns at low incidences than the Livox.

4.3 Real-world performance of the Livox AVIA

The real-world Livox scans confirm the general trends observed in the VLS simulations but reveal several practical limitations. The effective range of the sensor in the beach–dune environment is approximately 100–150 m. If we compare the number of returns per range vs. incidence angle combination (Figure 6), it becomes apparent that beyond this distance, returns become increasingly sparse, particularly for surfaces with incidence angles below 20°. The proportion of valid returns drops steeply with increasing range and decreasing incidence angle, indicating that the Livox is not well capable of detecting weak reflections from nearly horizontal sand surfaces.

The real-world Livox scans achieve a coverage of 42%, compared to 51–56% in the VLS simulations, a gap of 10–14 %. Spatially, this gap is concentrated in two types of areas, each linked to a specific terrain characteristic, as visible in Figure 4a.

The first type concerns low-slope regions at low incidence angles. In the region shown in Figure 4b, LIVOX-REAL only returns data over surfaces with relatively large local slope (e.g. car tracks in the sand; Figure 4c), whereas LIVOX-VLS shows coverage across the entire surface. This indicates that VLS overestimates backscatter at low incidence angles.

The second type concerns areas occluded by local dune topography. In the region shown in Figure 4d, LIVOX-REAL shows a larger gap in coverage that is not predicted by LIVOX-VLS. As visible in Figure 7, an elevated dune form along the line from P5 toward this region likely blocked part of the laser beams in the real-world scans. This might be related to the highly elliptical beam of the Livox AVIA, which is elongated in the vertical direction. When such a beam grazes a dune crest, its vertical extent increases the likelihood that part of the beam intersects the crest surface rather than passing over it entirely. This would cause more beam energy to be reflected at the crest, reducing illumination of the area behind it, which would not happen in a narrower circular beam approximation in HELIOS++. Additionally, slight variations in actual and simulated scanner position and height, or the simplification of the topography before simulation, removing very local elevation changes from, e.g., branches of bushes, are potential causes for this discrepancy.

5. Discussion

5.1 Suitability of Livox AVIA for permanent monitoring

The results indicate that multiple low-cost Livox AVIA sensors can achieve comparable coverage to that of a single high-end RIEGL VZ-2000i sensor in a permanent monitoring setup, though simulated low-cost sensors slightly overestimate real-world coverage. The latter could also be the case for the high-end sensor, of which the simulations have not been validated.

There is a trade-off in point density between the considered low-cost and high-end setups. The higher and more homogeneous point density over the AOI in the low-cost setups could be

This contribution has been peer-reviewed. The double-blind peer-review was conducted on the basis of the full paper.
https://doi.org/10.5194/isprs-annals-XI-1-2026-91-2026 | © Author(s) 2026. CC BY 4.0 License.

Scenario	Coverage (%)	Mean point density (pts/m^2)	Mean incidence angle (°)
LIVOX-VLS, *a*	52	968	12
LIVOX-VLS, *b*	56	1275	12
LIVOX-REAL	42	440	15
RIEGL-VLS	55	103	4

Table 1. Performance metrics of the different scanning scenarios. Since HELIOS++ only supports circular but not elliptical beam divergence, simulations are conducted with circular beam divergence using the semi-minor axis (a) and the mean of the semi-minor and the semi-major axis (b), both with the maximum raster representation. Simulated and real-world Livox AVIA scans are based on a scan duration of 20 s.

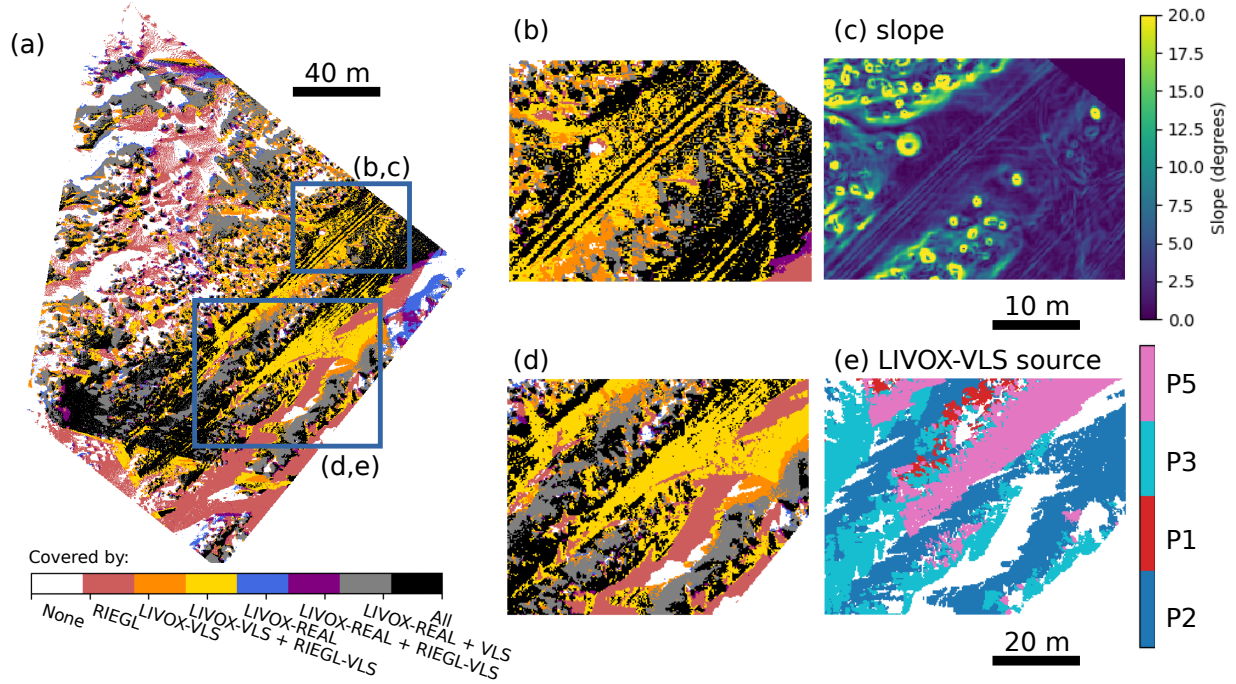

Figure 4. (a) Coverage of AOI in different scenarios. LIVOX-VLS is based on 20 s, with beam mode *b* (mean divergence); (b) and (d) zooms on areas where LIVOX-VLS obtains points but real-world scans do not; (c) slope of region in (b); (e) most common source ID per grid cell in LIVOX-VLS of region in (d).

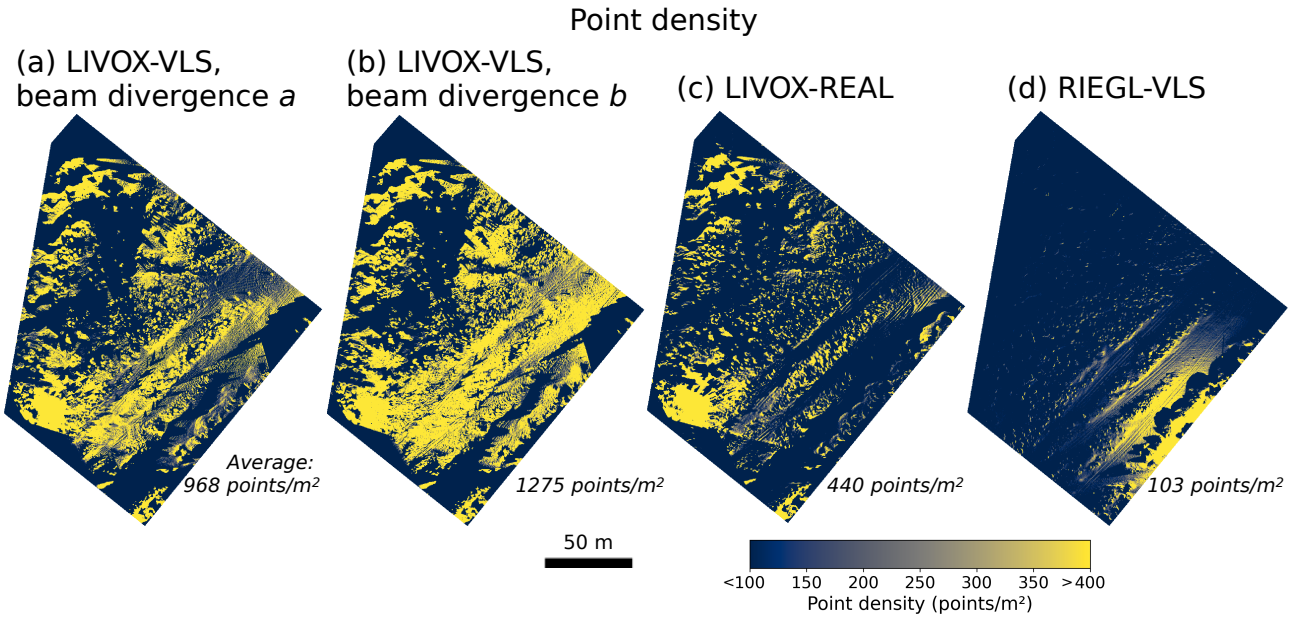

Figure 5. Point density over the AOI per selected scanning scenario.

This contribution has been peer-reviewed. The double-blind peer-review was conducted on the basis of the full paper.
https://doi.org/10.5194/isprs-annals-XI-1-2026-91-2026 | © Author(s) 2026. CC BY 4.0 License.

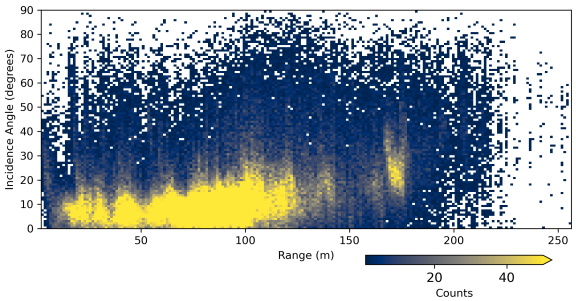

Figure 6. Count per range vs. incidence angle bin for the real world Livox scans (LIVOX-REAL). Incidence angle is based on the topography of the UAV-LiDAR (ULS) data.

exploited for targeted monitoring systems, for example, quantifying patterns of variations in cross-sectional beach-dune sand transport. That is, if the incidence angle and range limitations of the sensors are taken into account. A fitting use case would be to monitor a small spatial area (a smaller part of this AOI) and using the sediment supply variations measured at high temporal resolution (minutes - hours) in this low-cost setup, to extrapolate and explain causal conditions of large scale morphological variations, measured in monthly/seasonal area-wide ULS acquisitions.

For area-wide morphological monitoring, the lower precision and limited range of the Livox AVIA constrain its direct replacement of high-end PLS scanners. However, the increased point density achievable with multiple low-cost units could offset the precision limitations when constructing averaged DEMs. Future work should quantify how differences in precision and point density propagate further into change-detection uncertainty, for instance by comparing the minimum detectable elevation change across repeated epochs and ranges (Soudarissanane et al., 2011; Milan et al., 2011; Bui and Glennie, 2023). This would require real-world comparison of the precision of the Livox AVIA and RIEGL VZ-2000i, which cannot yet be assessed reliably through simulation only. Such analysis would clarify whether the increased noise level of low-cost scanners is acceptable for detecting morphological evolution at sub-decimetre scales, given the increased point density observed. Additionally, although its scanning mechanism is well-understood and has been simulated and applied successfully (Tabernig et al., 2025a,b), virtual RIEGL VZ-2000i scans should be directly compared to their real-world counterpart in a controlled coastal setting. Such validation, combined with a purely real-world comparison of the single-position RIEGL VZ-2000i and multi-position Livox AVIA setups, would allow further confirmation of the findings presented here.

5.2 Implications for PLS system design

Designing permanent laser scanning monitoring networks using low-cost sensors requires adequate decision-making for optimising spatial coverage, integration time, and scanning height + direction. The experiments show that a scanning duration of 10-20 s is quite sufficient for saturating the projected FOV of the Livox AVIA sensor. With longer durations, no great coverage improvements are made. Shorter scanning durations might be sufficient when monitoring very rapid sediment transport like the sand flux volume in a saltation layer, but this does diminish the coverage and point density. Simultaneous observations from different viewing angles could mitigate this lack of cover-

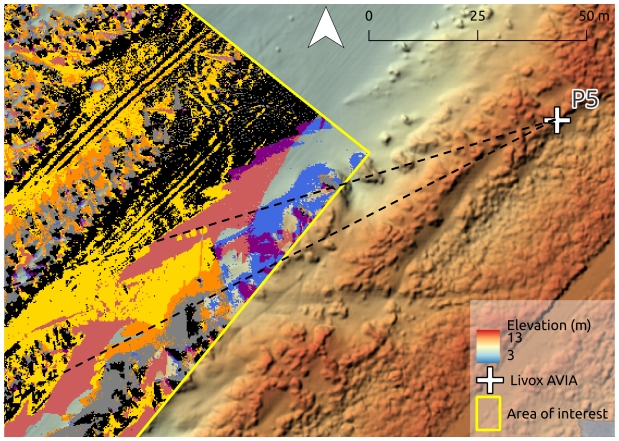

Figure 7. DEM of part of the AOI around scanning position P5, derived from the ULS data. Colors refer to the coverage as defined in Figure 4. The black dashed lines indicate the outer radial edges of the region lacking LIVOX-REAL data from P5, but containing simulated data from LIVOX-VLS.

age and point density, provided that inter-sensor timing is well synchronized.

The fact that only ∼50% of the area is covered in both low-cost and high-end setups highlights the critical role that scanning geometry and occlusion play in setup design. The elevated position (8 m) of the RIEGL VZ-2000i leads to smaller occluded areas behind dunes, and improves incidence angles. However, such larger poles are pricier and more invasive, thus when setting up a network with larger amount of scanners this is not preferred. Even so, elevating the measurement heights by a couple of meters could already largely decrease the occlusion and improve incidence angles of the low-cost setups. Furthermore, applying rotational ability (Výbošťok et al., 2025) to scan sequentially in different scanning directions could also reduce blind zones within the AOI, and increase point density homogeneity.

Permanent application of these low-cost setups also requires robust registration and temporal synchronisation of per-epoch and between-epoch scans. The manual alignment of dune crests in this study is adequate when considering coverage differences between setups, but when accurate change detection is required, more precise alignment is needed. In particular, when poles and scanners might move during intense weather conditions (Kuschnerus et al., 2021b). The lack of stable planar features in these beach-dune systems do hinder application of many established methods. Solutions could be the use of fixed targets or prisms, though this requires careful consideration of placement and size, and these targets could also move or get buried under sand. Other solutions could be automated dune crest detection (Lindenbergh et al., 2025b) and consecutive graph-based matching (Bot et al., 2019); or co-registration based on internal IMU observations (Kuschnerus et al., 2024).

Beyond their technical characteristics, the main advantage of low-cost sensors lies in their affordability. A single Livox AVIA unit costs on the order of a few thousand euros, approximately one-hundredth of the price of a high-end RIEGL VZ-2000i. This substantial price difference makes it economically feasible to deploy multiple scanners within the budget of a single high-end system, enabling denser and more frequent, multi-view observations in permanent monitoring networks.

This contribution has been peer-reviewed. The double-blind peer-review was conducted on the basis of the full paper.
https://doi.org/10.5194/isprs-annals-XI-1-2026-91-2026 | © Author(s) 2026. CC BY 4.0 License.

Establishing such a network of sensors requires careful consideration of power supply, data management, and connectivity. In the current setup, each AVIA is controlled by a Raspberry Pi and powered by batteries. The Raspberry Pi enables scheduling of scans and adjustment of scanning duration, with data presently stored locally. For a permanent installation, autonomous recharging or direct power supply will be essential. Power consumption measurements indicate that, although dependent on weather conditions, small solar panels could provide sufficient energy for both data acquisition and battery charging. In this study area, and likely in much of the Netherlands, telecommunication networks would permit wireless data transfer and remote management, though this may be more challenging in remote or infrastructure-limited regions. Future work should include a formal power budget analysis, incorporating measured power consumption of the Livox AVIA and Raspberry Pi under operational conditions, solar irradiance estimates for the deployment region, and battery sizing calculations, to provide concrete guidance for permanent autonomous installations.

The long-term durability of low-cost sensors in harsh coastal environments also requires further attention. The coast often exposes sensors to wind, windblown sand particles, and salt spray, all of which may degrade optical surfaces, mechanics, or electronic parts. Protective housing, such as those employed in the CoastScan setup (Vos et al., 2023), could be adapted for low-cost sensors to extend operational lifetime. Furthermore, the stability of sensor mounts in dynamic sand is a concern for long-term co-registration as poles may tilt over months to years if they are not anchored properly. Regular monitoring of pole stability, combined with robust automated co-registration strategies, are thus essential for reliable permanent deployments.

5.3 Reliability of Virtual Laser Scanning

VLS is shown to be effective for predicting performance trends between low-cost and high-end setups in terms of their coverage and range-dependent point density variations. Some discrepancies between the VLS and the actual data do highlight the need for consideration of current limitations when designing and validating the permanent monitoring setups.

HELIOS++ models only circular beam divergence, whereas the strongly elliptical beam of the Livox AVIA affects backscatter intensity and interacts with the anisotropic scanning pattern of the sensor. Until this factor is incorporated, it is important to consider both worst-case (semi-major axis) and best case (semi-minor axis) beam divergence when designing permanent monitoring setups with the Livox AVIA.

In the simulations, we limited the maximum range to 150 m and this threshold is applied uniformly over the FOV. The effective detection range of the Livox AVIA is however highest at the center of the FOV and decreases towards the edge (LIVOX AVIA User Manual, 2020). Integrating such variable effective detection ranges into the simulations or the post-processing could improve the agreement of simulated and real-world data.

Furthermore, the representation of the topography in the simulation can strongly influence occlusion and backscatter estimation. A maximum raster of 0.1 m cell size provided more realistic coverage percentage than a detailed mesh, but still seemingly did not capture all topographic inference possible for incoming laser beams. Even higher resolution representation could prove to make the VLS closer to reality, but this does require more intense computation.

Additional considerations that might have caused the variations in performance between simulated and real data are the effects of surface reflectance and atmospheric scattering. Intermittent raining and consequent increase in soil and atmospheric moisture during real-world scanning, as recorded by the Dutch Royal Meteorological Institute at Hoek van Holland (KNMI, 2025, Station 330), possibly increased absorption of the laser beam, and thus reduced backscatter intensity and potential, especially at lower incidence angles (Di Biase et al., 2021). The reduced backscatter intensity, and consequent reduction of measured returns, under different conditions and surface properties, could in future work be more accurately be modeled with HELIOS++ through calibration of the echo detection thresholds.

6. Conclusions

This study assesses the feasibility of using multiple low-cost Livox AVIA sensors as an alternative to a single high-end RIEGL VZ-2000i scanner, for PLS of sandy beach-dune systems. VLS simulations using HELIOS++ are combined with field measurements to evaluate both sensor performance and the ability of VLS to represent real-world setups. In this way, we showcase the ability of VLS to aid future setup design and identify the most promising setups to be tested in the field.

The results show that a configuration of several Livox AVIA sensors can reach a similar overall coverage to that of the high-end system at a substantially lower price, although the real-world data indicates slightly lower performance than the simulations in terms of point density and coverage. Effective range and incidence angle limitations (100-150 m) seemingly restrict the suitability of the Livox AVIA for direct area-wide application, but the higher and more uniform point density when using multiple sensors offers the potential for local, very high frequency (seconds-minutes) 3D monitoring of morphological change. The larger point density of the Livox AVIA could also partially compensate for the reduced range precision compared to the RIEGL VZ-2000i, depending on the required topographical scale for surface reconstruction, although assessing this would require further real-world verification and comparison of the RIEGL VZ-2000i.

The VLS simulations are found to realistically reproduce overall coverage patterns and spatial point density distribution, but tend to overestimate returns at low-incidence angles and underestimate occlusion potential of the terrain. This variation likely results from the circular beam approximation in HELIOS++, as well as from unmodelled detail in the virtually scanned digital representation, and moisture effects on the surface and atmosphere. Future developments should thus focus on incorporating this elliptical beam divergence, and moisture effects to further improve the accuracy of the simulated results. Additionally, future applications should carefully regard worst-case and best-case scenarios of terrain representation as well as beam divergence.

7. Acknowledgements

This publication is part of the project AdaptCoast with file number 20014 of the research programme Open Technology Programme which is (partly) financed by the Dutch Research Council (NWO) under the grant 20014. This work was also supported by the Deutsche Forschungsgemeinschaft (DFG, German Research Foundation) in the frame of the project ”Vir-

tuaLearn3D” (project no. 496418931), and the project ”Fostering a community-driven and sustainable HELIOS++ scientific software” (no. 528521476).

We are also thankful to M. Ahmed, A. De Jong, F. The, for their assistance during the fieldwork.

References

Anders, K., Winiwarter, L., Mara, H., Lindenbergh, R., Vos, S. E., Höfle, B., 2021. Fully automatic spatiotemporal segmentation of 3D LiDAR time series for the extraction of natural surface changes. *ISPRS Journal of Photogrammetry and Remote Sensing*, 173, 297–308. 10.1016/j.isprsjprs.2021.01.015.

Bi, S., Yuan, C., Liu, C., Cheng, J., Wang, W., Cai, Y., 2021. A Survey of Low-Cost 3D Laser Scanning Technology. *Applied Sciences*, 11(9), 3938. 10.3390/app11093938.

Bot, F. J., Nourian, P., Verbree, E., 2019. A GRAPH-MATCHING APPROACH TO INDOOR LOCALIZATION USING A MOBILE DEVICE AND A REFERENCE BIM. *The International Archives of the Photogrammetry, Remote Sensing and Spatial Information Sciences*, XLII-2/W13, 761–767. 10.5194/isprs-archives-XLII-2-W13-761-2019.

Bui, L. K., Glennie, C. L., 2023. Estimation of lidar-based gridded DEM uncertainty with varying terrain roughness and point density. *ISPRS Open Journal of Photogrammetry and Remote Sensing*, 7, 100028. 10.1016/j.ophoto.2022.100028.

Chowdhury, P., Lakku, N. K. G., Lincoln, S., Seelam, J. K., Behera, M. R., 2023. Climate change and coastal morphodynamics: Interactions on regional scales. *Science of The Total Environment*, 899, 166432. 10.1016/j.scitotenv.2023.166432.

De Bruijne, A., Van Buren, J., Kösters, A., Van Der Marel, H., 2005. *Geodetic reference frames in the Netherlands*. Nederlandse Commissie voor Geodesie.

De Schipper, M. A., De Vries, S., Ruessink, G., De Zeeuw, R. C., Rutten, J., Van Gelder-Maas, C., Stive, M. J., 2016. Initial spreading of a mega feeder nourishment: Observations of the Sand Engine pilot project. *Coastal Engineering*, 111, 23–38. 10.1016/j.coastaleng.2015.10.011.

De Vugt, L., Carraro, E., Fatihi, A., Mattea, E., Myall, E., Czerwonka-Schröder, D., Anders, K., 2025. Permanent Laser Scanning and 3D Time Series Analysis for Geomorphic Monitoring using Low-Cost Sensors and Open-Source Software. *The International Archives of the Photogrammetry, Remote Sensing and Spatial Information Sciences*, XLVIII-G-2025, 359–365. 10.5194/isprs-archives-XLVIII-G-2025-359-2025.

Di Biase, V., Hanssen, R. F., Vos, S. E., 2021. Sensitivity of Near-Infrared Permanent Laser Scanning Intensity for Retrieving Soil Moisture on a Coastal Beach: Calibration Procedure Using In Situ Data. *Remote Sensing*, 13(9), 1645. 10.3390/rs13091645.

Hulskamp, R. L., Pregnolato, M., De Vries, S., 2025. Dynamics of engineered coastal dune landscapes at the Zandmotor. *Discover Geoscience*, 3(1), 244. 10.1007/s44288-025-00360-x.

Hulskemper, D., Antolínez, J. A. , Lindenbergh, R., Anders, K., 2026. Coastal process understanding through automated identification of recurring surface dynamics in permanent laser scanning data of a sandy beach. *Earth Surface Dynamics*, 14(3), 329–359. 10.5194/esurf-14-329-2026.

KNMI, 2025. Uurgegevens van het weer in Nederland. https://www.knmi.nl/nederland-nu/klimatologie/uurgegevens.

Kuschnerus, M., De Vries, S., Antolínez, J. A., Vos, S., Lindenbergh, R., 2024. Identifying topographic changes at the beach using multiple years of permanent laser scanning. *Coastal Engineering*, 193, 104594. 10.1016/j.coastaleng.2024.104594.

Kuschnerus, M., Lindenbergh, R., Vos, S., 2021a. Coastal change patterns from time series clustering of permanent laser scan data. *Earth Surface Dynamics*, 9(1), 89–103. 10.5194/esurf-9-89-2021.

Kuschnerus, M., Schröder, D., Lindenbergh, R., 2021b. ENVIRONMENTAL INFLUENCES ON THE STABILITY OF A PERMANENTLY INSTALLED LASER SCANNER. *The International Archives of the Photogrammetry, Remote Sensing and Spatial Information Sciences*, XLIII-B2-2021, 745–752. 10.5194/isprs-archives-XLIII-B2-2021-745-2021.

Lindenbergh, R., Anders, K., Campos, M., Czerwonka-Schröder, D., Höfle, B., Kuschnerus, M., Puttonen, E., Prinz, R., Rutzinger, M., Voordendag, A., Vos, S., 2025a. Permanent terrestrial laser scanning for near-continuous environmental observations: Systems, methods, challenges and applications. *ISPRS Open Journal of Photogrammetry and Remote Sensing*, 17, 100094. 10.1016/j.ophoto.2025.100094.

Lindenbergh, R., Dewez, T., Hulskemper, D., 2025b. Assessing 3D morphological dune changes using medial axes. *Proceedings of the 6th Joint International Symposium on Deformation Monitoring - JISDM 2025*. 10.5445/IR/1000179777.

LIVOX AVIA User Manual, 2020. `https://terra-1-g.djicdn.com/65c028cd298f4669a7f0e40e50ba1131/Download/Avia/Livox%20Avia%20User%20Manual%20202022 04.pdf`.

Milan, D. J., Heritage, G. L., Large, A. R., Fuller, I. C., 2011. Filtering spatial error from DEMs: Implications for morphological change estimation. *Geomorphology*, 125(1), 160–171. 10.1016/j.geomorph.2010.09.012.

Riegl VZ-2000i Data sheet, 2019. `https://www.riegl.com/fileadmin/media/Products/01_Terrestrial_Scanning/RIEGL_VZ-2000i/RIEGL_VZ-2000i_Datasheet_2025-09-16.pdf`.

Ruttner-Jansen, P., Glaus, J., Wieser, A., Bühler, Y., 2023. A MEASUREMENT SYSTEM FOR MAPPING SNOW DISTRIBUTION CHANGES IN AN AVALANCHE RELEASE ZONE. *International Snow Science Workshop Proceedings 2023*, Montana State University Library, Bend, OR, USA.

Schröder, D., Anders, K., Winiwarter, L., Wujanz, D., 2022. Permanent terrestrial LiDAR monitoring in mining, natural hazard prevention and infrastructure protection – Chances, risks, and challenges: A case study of a rockfall in Tyrol, Austria. *Proceedings of the 5th Joint International Symposium on Deformation Monitoring - JISDM 2022*. 10.4995/JISDM2022.2022.13649.

Soudarissanane, S., Lindenbergh, R., Menenti, M., Teunissen, P., 2011. Scanning geometry: Influencing factor on the quality of terrestrial laser scanning points. *ISPRS Journal of Photogrammetry and Remote Sensing*, 66(4), 389–399. 10.1016/j.isprsjprs.2011.01.005.

Stive, M. J., De Schipper, M. A., Luijendijk, A. P., Aarninkhof, S. G., Van Gelder-Maas, C., Van Thiel De Vries, J. S., De Vries, S., Henriquez, M., Marx, S., Ranasinghe, R., 2013. A New Alternative to Saving Our Beaches from Sea-Level Rise: The Sand Engine. *Journal of Coastal Research*, 290, 1001–1008. 10.2112/JCOASTRES-D-13-00070.1.

Tabernig, R., Albert, W., Weiser, H., Fritzmann, P., Anders, K., Rutzinger, M., Höfle, B., 2025a. Temporal aggregation of point clouds improves permanent laser scanning of landslides in forested areas. *Science of Remote Sensing*, 100254. 10.1016/j.srs.2025.100254.

Tabernig, R., Albert, W., Weiser, H., Höfle, B., 2025b. A hierarchical approach for near real-time 3D surface change analysis of permanent laser scanning point clouds. *Proceedings of the 6th Joint International Symposium on Deformation Monitoring - JISDM 2025*. 10.5445/IR/1000180377.

Vos, S., Anders, K., Kuschnerus, M., Lindenbergh, R., Höfle, B., Aarninkhof, S., De Vries, S., 2022. A high-resolution 4D terrestrial laser scan dataset of the Kijkduin beach-dune system, The Netherlands. *Scientific Data*, 9(1), 191. 10.1038/s41597-022-01291-9.

Vos, S., Kuschnerus, M., Lindenbergh, R., de Vries, S., 2023. 4D spatio-temporal laser scan dataset of the beach-dune system in Noordwijk, NL. https://data.4tu.nl/datasets/1aac46fb-7900-4d4c-a099-d2ce354811d2/2.

Výbošťok, J., Chudá, J., Tomčík, D., Gretch, D., Tomaštík, J., Pełka, M., Mokroš, M., 2025. An Open and Low-Cost Terrestrial Laser Scanner Prototype: Delivering Reliable Accuracy for Forest Practice on a Budget.

Winiwarter, L., Esmorís Pena, A. M., Weiser, H., Anders, K., Martínez Sánchez, J., Searle, M., Höfle, B., 2022. Virtual laser scanning with HELIOS++: A novel take on ray tracing-based simulation of topographic full-waveform 3D laser scanning. *Remote Sensing of Environment*, 269, 112772. 10.1016/j.rse.2021.112772.